Computer-Aided Design and Applications

3D Shape Reasoning for Identifying Anatomical Landmarks

K. Subburaj[1], B. Ravi[1] and M. G. Agarwal[2]

[1]Indian Institute of Technology Bombay, {subburaj,b.ravi}@iitb.ac.in
[2]Tata Memorial Hospital Mumbai, mgagarwal@gmail.com

ABSTRACT

Orthopaedic surgeries require identification of anatomical landmarks on skeletal tissue. Manual palpation methods may not be accurate, especially in resecting deceased tissue and positioning custom implants or mega endo-prostheses. This article describes a computer-aided method for automatic identification of anatomical landmarks on a 3D model reconstructed from CT images of the patient. This is based on computing curvature values, identifying different regions of the surface (generated from the segmented volume data), and classifying the regions as peaks, ridges, pits and ravines. The landmarks are identified by walking along all vertices, extracting gradients from curvature map, and checking against a set of rules. The approach has been successfully demonstrated on a pelvis model reconstructed from 443 slices. The locations of the landmarks are determined, useful for dimension measurements and pre-operative planning.

Keywords: anatomical landmarks, curvature and its derivatives, pre-operative planning.
DOI: 10.3722/cadaps.2008.153-160

1. INTRODUCTION

Anatomical landmarks are distinct regions or points with uniqueness in shape characteristics in their vicinity. Figure 1 shows typical landmarks on a pelvis. In contrast to fiducial markers that are placed on body surface, anatomical landmarks have the advantage of being located inside the body, thereby increasing the accuracy of surgical intervention. They are also required for pre-operative planning and custom implant design. Manual location of anatomical landmarks is however, time consuming and may lack in accuracy. These limitations can be overcome by automated or semi-automated procedures with computer assistance.

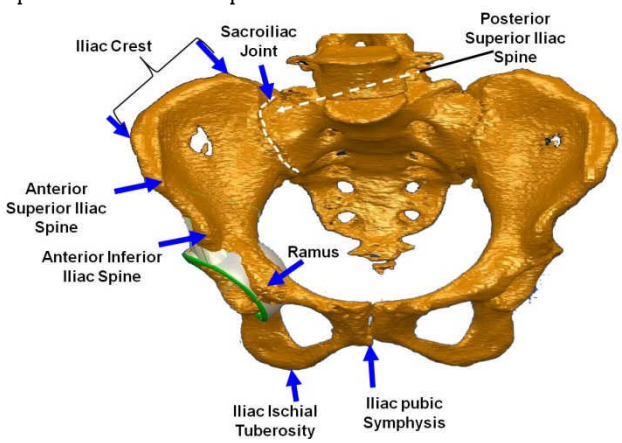

Fig. 1: Major pelvis landmarks used during surgery.

A primary reason for the positional uncertainty of anatomical landmarks is the fact that they are not clearly identifiable discrete points, but are rather relatively large and curved areas. Prior knowledge on anatomical landmarks is necessary to locate and identify them precisely [2]. Most landmarks are palpable or referred with respect to another palpable landmark. Geometric characteristics such as curvatures, extreme points, and higher order derivatives can be used for classifying regions of bone surface as landmarks.

The following section presents related work in characterisation of geometric landmarks, followed by our proposed two stage methodology to identify anatomical landmarks, demonstrated on a pelvis model. The paper concludes with further work in this direction.

2. RELATED WORK

A comprehensive list of lower limb landmarks and palpation procedures for locating the landmarks have been described by Jan [7]. Viceconti et al. [15] used interactively identified anatomical landmarks on 3D virtual model for aligning medullary prosthesis. Croce et al. [3] carried out studies in manual location of lower limb landmarks by different surgeons, and found that the variations are in the range 6-25 mm. In general, manual location of landmarks and related measurements are a time consuming process and require a high level of expertise. Identification of anatomical landmarks from 3D laser digitized data [10] or CT images scanned with optical or metal markers on object [5], are highly sensitive to the orientation and position of the patient during scan. The method of using fiducial markers for prosthesis positioning and registration may not always be feasible. The movement of muscle and skin during scanning also affects the result. It is preferable to locate the landmarks on skeletal surface, since they are independent of patient's position and orientation.

Surface curvature is independent of position and orientation of patients and it can help in reliable detection of geometric features, from which landmarks can be derived. Maekawa et al [11] used curvature to classify surface into various regions such as umbilics and singular lines. Page et al [12] used a normal voting method and coefficients derived from principal curvatures in identifying crest lines. Razdan and Bae [13] combined watershed and vertex based approaches driven by surface characteristics to classify regions on triangular mesh. Drerup and Hierholzer [4] identified lumbar dimples based on surface curvature, and used it to study spine shape and muscle movement over pelvis. Griffin et al. [6] studied the anatomy of condyle landmarks and their usefulness in measuring critical dimensions and positioning of implants during surgery using MRI images. Ehrhardt et al [5] proposed an approach to measure dimensions on a triangulated hip model, by fitting similar simple geometric shapes over identified landmark regions.

In summary, manual localisation of anatomical landmarks may not be accurate nor robust. Landmark identification based on 3D digitising of outer body surface or CT scan of synthetic bone model are also not reliable owing to errors caused by movement of skin, or that of patient during scanning, respectively. We therefore propose an approach for identifying landmarks driven by *curvature analysis and rules*. For this purpose, different regions of the surface are classified as peaks, ridges, pits and ravines, as described next.

3. GEOMETRICAL LANDMARKS

Geometrically invariant measures useful for identifying anatomical landmarks on a 3D anatomical model are presented here. This includes four most common geometric shapes: *peak*, *ridge*, *pit*, and *ravine* (Fig. 2), observed in regard to the anatomical landmarks used in orthopaedic surgery.

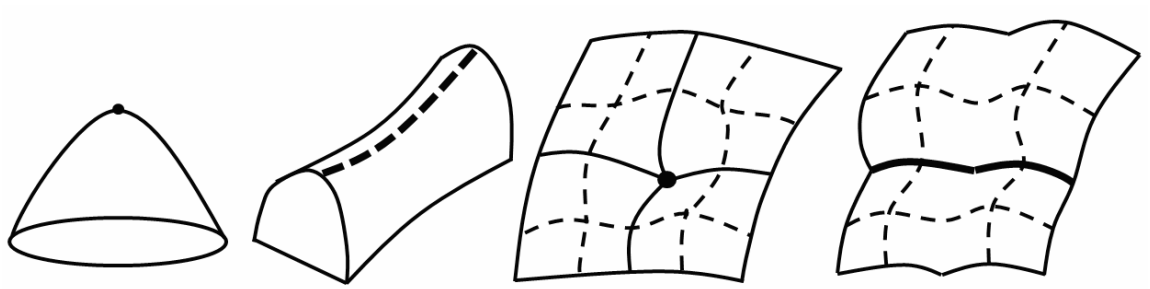

Fig. 2: Geometric landmarks: peak, ridge, pit, and ravine.

3.1 Peak and Ridge

A peak and ridge are n-2 dimensional elements of an n-dimensional polytope. A peak can be described as a point with local maximum real-valued function and high gradient with respect to surroundings. A ridge is a narrow, raised strip of line formed by the juncture of two sloping surfaces diverging towards the ground. In its broadest sense, the notion of peak and ridge generalizes the idea of a local maximum of a real-valued function such as curvature and its derivatives.

A point X_0 in the domain of a function $f = \mathbb{R}^3 \rightarrow \mathbb{R}$ is a local maximum of the function. There is a distance $\delta > 0$ with the property that if X is within δ units of X_0, then $f(X) > f(X_0)$. Consider the condition that $f(X) > f(X_0)$ for X in an entire neighbourhood of X_0. This enables collecting the set of points which satisfy the above criteria, to form a 1-dimensional locus or isolated region, it is labelled as a peak and if it forms a curve, it is labelled as a ridge.

3.2 Pit and Ravine

A pit and ravine have a similar characteristic that they represent a local minimum of an intrinsic real-valued function. Pit is a point surrounded by a high walled locally depressed region on surface. A ravine can be defined as a line formed by intersection of two concave surfaces.

It is well known that critical points, of which local minima are just one type, are isolated points or curves in a function's domain. A point X_0 in the domain of a function $f = \mathbb{R}^3 \rightarrow \mathbb{R}$ is a local minimum of the function if there is a distance $\delta > 0$ with the property that if X is within δ units of X_0, then $f(X) < f(X_0)$. Consider the condition that $f(X) < f(X_0)$ for X in an entire neighbourhood of X_0, which allows identifying the set of points satisfying the above criteria. If the set forms a one dimensional locus or isolated region, it is labelled as a pit. If it forms a curve, it is labelled as a ravine.

4. METHODOLOGY

The overall methodology for identifying anatomical landmarks is shown in figure 3. First a 3D surface model is reconstructed from a set of CT images [14]. Then principal curvatures and their derivatives are computed on every vertex of the triangulated surface. These vertices are classified based on the curvature descriptors into various regions. Thereafter anatomical landmarks are identified from these regions by pre-defined rules. The detailed methodology is described below.

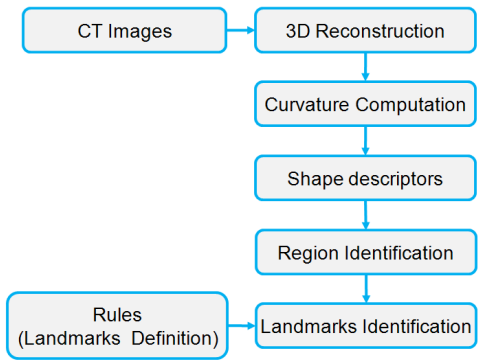

Fig. 3: Overview of the methodology for landmarks identification.

4.1 Curvature Estimation

Curvature estimation requires triangulated surface data, produced by surface fitting on volumetric data reconstructed from CT images. The Gaussian curvature of a vertex v in a irregular surface with a polyhedral metric can be calculated. Let x_i be the three-dimensional coordinate vectors of the vertices v_i=1, …, n, adjacent to v $v \in T$, T be the set of triangles and x be the coordinate vector of v. The reduced form of Gauss-Bonnet approach [1], which uses the angle α_i at v and two successive edges (Fig. 4) for polygonal meshes, is given as

$$\iint_A K dA = 2\pi - \sum_{i=0}^{n-1} \alpha_i$$

The geometric flow of the surface must be integrated with vertices which will be updated according to the average behaviour of the surface around it. Therefore, the piecewise linear result of the flow will be an appropriate approximation of the smoothed surface. Since we made no assumption on the smoothness of the surface, we will restrict the average to be within the immediate neighbouring triangles. We define the discrete Gaussian curvature, k_G, at a vertex v as:

$$k_G = \frac{1}{A}\iint_A K dA$$

where A is the accumulated area of all triangles around vertex v. The mean curvature k_H is defined as the average of the normal curvatures:

$$k_H = \frac{1}{2\pi}\int_0^{2\pi} k_N(\theta)\, d\theta$$

Expressing the normal curvature in terms of the principal curvatures, $k_N(\theta) = k_{\min}\cos^2(\theta) + k_{\max}\sin^2(\theta)$ leads to the well-known definition of mean curvature $k_H=(k_{min}+k_{max})/2$. The calculated minimum and maximum principle curvature values (K_{min} and K_{max}) are in corresponding principal directions (t_{min} and t_{max}) respectively, which are orthogonal.

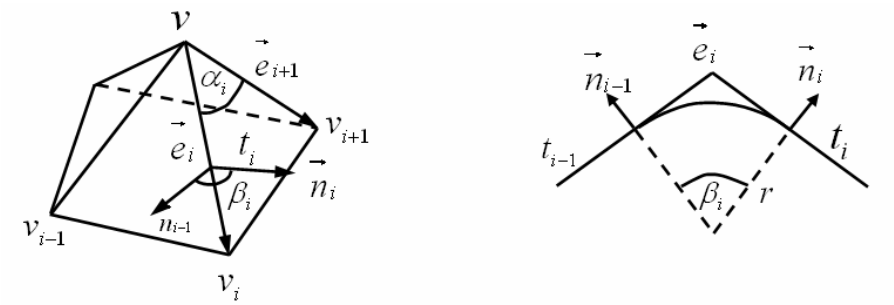

Fig. 4: Neighbourhood surface regions and curvature computation from triangular mesh

4.2 Region Identification

The derivatives based on principal curvatures are used as descriptors to decide whether a vertex belongs to a landmark region or not. The descriptors based on principal curvatures given by Koenderink [9] are as follows.

Shape Index captures the local shape in a range of [-1, +1]: $\eta = 1/2 - (1/\pi)\tan^{-1}\left((k_1+k_2)/(k_1-k_2)\right)$

Curvedness is a positive number that specifies the amount of curvature: $k = \sqrt{(k_1^2+k_2^2)/2}$

The other two descriptors are $S_{\min} = \Delta K_{\min}/\Delta t_{\min}$ and $S_{\max} = \Delta K_{\max}/\Delta t_{\max}$. We call them principal coefficients, as they define the extremities. If one of the principal coefficients vanishes or falls below a threshold value, then it provides a hint of the landmarks such as ridges and ravines.

If $S_{min}=0$, $S_{\max} = \Delta K_{\max}/\Delta t_{\max} < 0$, and $K_{\max} > |K_{\min}|$ then the vertex belongs to a ridge.

If $S_{max}=0$, $S_{\min} = \Delta K_{\min}/\Delta t_{\min} > 0$, and $K_{\min} < -|K_{\min}|$ then the vertex belongs to a ravine.

The 3D model surface is colour coded and divided into regions according to geometric characteristics. High curvatures are coloured red, whereas low (negative) curvatures are coloured blue. Thus red islands indicate peaks, red lines indicate ridges, blue islands indicate pits, and blue lines indicate ravines. Then we map the numerical (quantitative) results of the curvature derivatives into qualitative terms such as high, medium, and low. These qualitative terms allow us to segment the surface into regions based on its homogeneity in specific characteristic. The regions are filtered based on their surface area to eliminate noise, and then tabulated to form a relationship matrix based on their location. The matrix can be evaluated by a set of rules for identifying landmarks (detailed in the next section).

4.3. Rules for Anatomical Landmarks

In general, we need not (in fact, cannot) detect every landmark, and the landmarks which we do detect may or may not be unique. We just need to identify enough landmarks to solve the application being tackled such as positioning of an implant. As of now, intra-operative assessment of landmarks is done based on the surgeon's experience. A specific landmark possesses the same set of geometric characteristics but varies in size and location depending on patient's age, gender, etc. This makes automatic identification of landmarks difficult, since two different landmarks may have similar geometric characteristics. We therefore propose an additional characteristic: relative position of a landmark with respect to other landmarks in its vicinity, for its identification. Rules have been formulated to characterise each landmark in terms of its shape and topology. For example, the rules for identifying anatomical landmarks of pelvis model are given below (refer to figure 1):

- ***Ramus*** is a prominent peak located on the anterior superior medial side of acetabulam centre, anterior superior lateral side of iliac pubic symphysis (IPY), near the boundary of acetabular ring.
- ***Iliac crest*** is a ridge located on top of the iliac bone, anterior superior and diagonal to the sacroiliac joint centre (virtual), superior anterior side of posterior superior iliac spine (PSIS), and superior posterior side of anterior superior iliac spine (ASIS).
- ***Anterior superior iliac spine (ASIS)*** is a sharp peak located on the anterior aspect of iliac crest on iliac bone, superior posterior diagonal side of anterior inferior iliac spine (AIIS), and exactly in line with the PSIS in medial and lateral side.
- ***Anterior inferior iliac spine (AIIS)*** is a peak located inferior to ASIS, lateral to ramus.
- ***Posterior superior iliac spine (PSIS)*** is a peak, less sharp than ASIS, located on the posterior side of iliac crest and diagonally inferior, and near to sacroiliac joint centre.
- ***Iliac ischial tuberosity (IIT)*** is a tuberosity (large peak) located at posteror-inferior aspect of the iliac bone, and anterior lateral diagonal to iliac pubic symphysis (IPY).
- ***Iliac pubic symphysis (IPY)*** is a peak located anterior side of iliac bone, medial to ramus.

5. IMPLEMENTATION AND RESULTS

The results are presented here for a pelvis reconstructed from 443 CT image slices. The CT images were imported in DICOM format, followed by filtering and segmentation to reconstruct a volumetric model of the bone (Fig. 5). This was converted into a surface model with 128,064 facets, using volumetric data surface tiling algorithm [8].

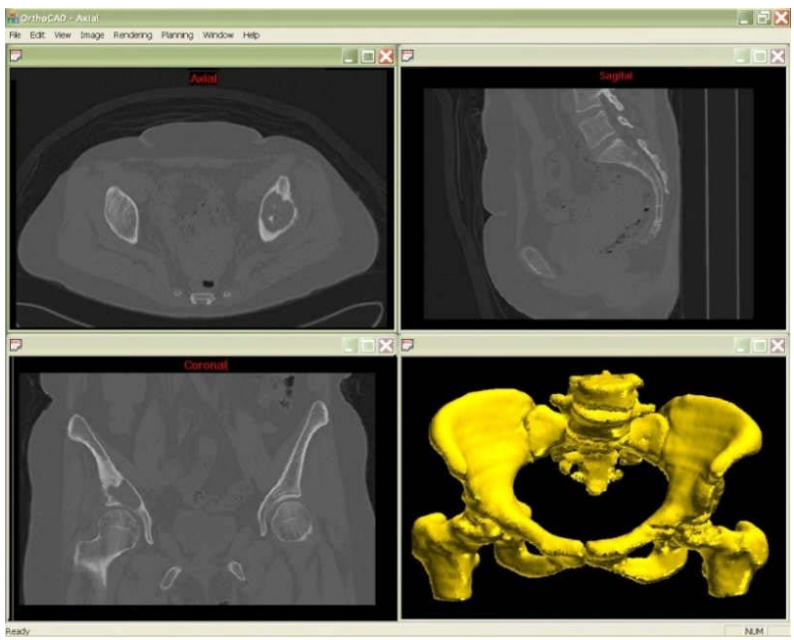

Fig. 5: Reconstructed pelvis bone model from CT images.

The curvatures and its derivative coefficients were computed to characterize the bone surface. Red and blue indicate regions with high and low (negative) curvature respectively, and green indicates smooth transition of curvature. Figure 6 shows the high curvature regions. Their boundaries are marked manually. The curvature computation took 73 seconds, and region classification took 139 seconds. Total memory occupied was 1282 MB.

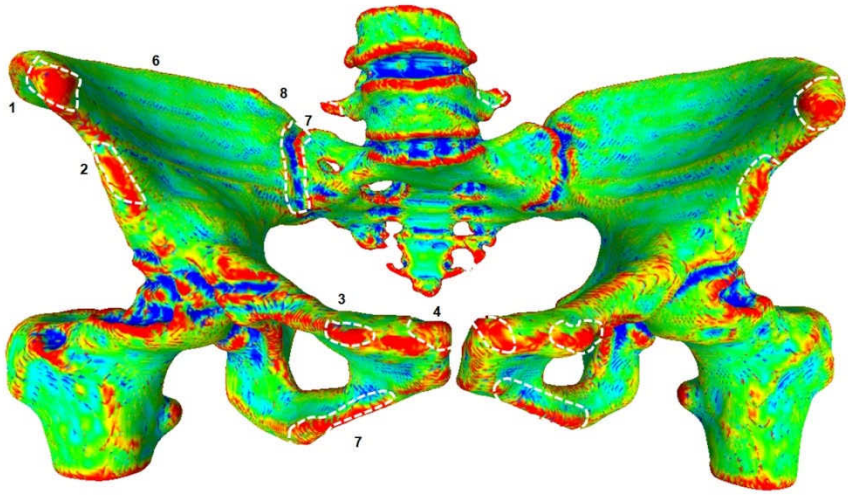

Fig. 6: Localised (highlighted) landmark regions of pelvis.

The location of a region is given by the median of the points in the region, and is used as its reference point. Its area gives an approximate indication of its size. The regions are stored temporarily as separate objects (Tab. 1), characterised as peak, ridge, pit, and ravine. A relationship matrix is formed between the regions based on their relative location (Tab. 2). This is evaluated by the landmark identification rules using geometric characteristics and topological relationships. For example, take landmark 1, which is a peak, located in line with landmark 5 ($\Delta z=0$), and located superior ($\Delta z=21$), posterior ($\Delta y=-38$), and lateral ($\Delta x=-31$) to landmark 2. These relations confirm that is ASIS as per the rules defined in section 4.3. Similarly, other identified landmarks are also identified. They are (2) AIIS, (3) Ramus, (4) IPY, (5) PSIS, (6) Iliac crest, (7) IIT, and (8) sacroiliac joint.

Landmark No	Type	Location	Area (mm^2)
1	Peak	(130, 191, 23)	1318.36
2	Peak	(99, 153, 44)	1286.59
3	Peak	(56, 198, 130)	922.78
4	Peak	(55, 196, 139)	860.81
5	Peak	(143, 20, 23)	594.68
6	Ridge	(195, 93, 32)	5798.92
7	Ridge	(14, 189, 120)	1506.19
8	Ravine	(146, 62, 98)	2486.89

Tab. 1: Parameters of the landmarks.

The 3D model reconstructed from CT images may have eroded surfaces and islands due to noise and defective tissue (ex. tumours). To reduce the error caused by the noise present in CT images, we incorporated a set of 2D image filters to reduce the noise and enhance the boundary pixels. Triangulation of volumetric data also affects the quality of surface data. 3D mesh filters are used to eliminate triangulation errors created during conversion of triangle surface data from volumetric data. This includes degeneracy, holes at a vertex, gaps along a line of intersection, and collapsed edges of small triangles. Unidentified errors in the model lead to identification of a large number of regions. These regions are filtered out by surface area check. The factors used in the calculation of curvature and local surface area can be adjusted to improve the accuracy of final location of landmarks.

Some of the landmarks, which are not labelled, are used as reference landmarks. These reference landmarks are derived from the identified anatomical landmarks and may positioned inside or outside the bone model, like a mid-point between two landmarks. For example, sacroiliac joint centre is identified with reference to PSIS and PIIS landmarks, and pubic symphysis centre is located at the midpoint between left IPY and right IPY. Anatomical and mechanical axis required for prosthesis positioning are also computed from identified landmarks.

LM	1	2	3	4	5	6	7	8
1	0,0,0	-31,-38,21	-74,7,107	-75,5,116	13,-171,0	65,-98,9	-116,-2,97	16,-129,75
2		0,0,0	-43,45,86	-44,43,95	44,133,21	96,-60,-12	-85,36,76	47,-91,54
3			0,0,0	-1,-2,9	87,-178,107	139,-105,-98	-42,-9,-10	90,-136,-32
4				0,0,0	88,-176,116	140,-103,-107	-41,-7,-19	91,-134,-41
5					0,0,0	52,73,-60	-129,169,28	3,42,6
6						0,0,0	-181,96,88	-49,-31,66
7							0,0,0	132,-127,-22
8								0,0,0

Tab. 2: Relationship matrix between landmarks.

6. CONCLUSION

In summary, we have presented an approach for identifying anatomical landmarks on 3D models reconstructed from CT images of the patient, unlike some previous approaches based on digitized point clouds or CT/MR images of synthetic models. It employs curvature for region identification, and rules for landmark identification on bones. The rules for landmark identification use curvature derivatives (curvature gradient, peaks, ridges, pits, and ravines), as well as topology (relative position) of identified regions. Since the identified landmarks are on bone rather on outer body surface, errors caused by skin movement and patient's position during data acquisition are minimised. The uniqueness of this approach is repeatability and accuracy of identifying landmarks regions and locations. This is ensured by various unique geometric characteristics of the chosen landmarks and topological relationship between landmarks.

Future work includes estimating various dimensions required in selecting suitable implant components, and for designing customised orthopaedic implants based on a set of rules formed in relation with the identified landmarks and required measurements. We also plan to use these landmarks for specifying markers location in intra-operative navigation, estimating deformities for prosthesis individualisation, and positioning prosthesis components based on the patient's anatomy.

7. ACKNOWLEDGEMENT

This work is a part of an ongoing project in OrthoCAD Network Research Centre at Indian Institute of Technology Bombay for developing a computer aided customised orthopaedic implant design and surgery planning system. It is supported by the Office of the Principal Scientific Adviser to the Government of India, New Delhi.

8. REFERENCES

[1] Agam, G.; Tang, X.: A Sampling Framework for Accurate Curvature Estimation in Discrete Surfaces, IEEE Transactions on Visualisation and Computer Graphics, 11(5), 2005, 573-583.

[2] Agarwal, M. G.; Anchan, C.; Shah, M.; Puri, A.; Pai, S.: Limb Salvage Surgery for Osteosarcoma: Effective Low-cost Treatment, Clinical Orthopaedics and Related Research, 459, 2007, 82-91.

[3] Croce, U. D.; Cappozzo, A.; Kerrigan, D. C.: Pelvis and Lower Limb Anatomical Landmark Calibration Precision and its Propagation to Bone Geometry and Joint Angles, Medical and Biological Engineering and Computing, 37, 1999, 155-161.

[4] Dreup, B.; Hierholzer, E.: Back Shape Measurement using Video Rasterstereography and 3D Reconstruction of Spinal Shape, Clinical Biomechanics, 9, 1994, 28-36.

[5] Ehrhardt, J.; Handels, H.; Strathmann, B.; Malina, T.; Plotz, W.; Poppl, S. J.: Atlas-based Recognition of Anatomical Structures and Landmarks to Support the Virtual Three-Dimensional Planning of Hip Operations, Lecture Notes in Computer Science, 2878, 2003, 17–24.

[6] Griffin, F. M.; Math, K.; Scuderi, G. R.; Insal, J. N.; Poilvache, P. L.: Anatomy of the Epicondyles of the Distal Femur MRI Analysis of Normal Knees, The Journal of Arthroplasty, 15(3), 2000, 354-359.

[7] Jan, S. V.: Skeletal Landmark Definitions, Technical Report, University of Brussels, 2004.
[8] Kay, P. A.; Robb, R. A.; Myers, R. P.; King, B. F.: Creation and validation of patient specific anatomical models for prostate surgery planning using virtual reality, Lecture Notes in Computer Science, 1131, 1996, 547-552.
[9] Koenderink, J.; Dooen, A. V.: Surface Shape and Curvature Scales, Image and Vision Computing, 10(8), 1992, 557-565.
[10] Liu, X.; Kim, W.; Drerup, B.: Foot 3D Characterization and Localization of Anatomical Landmarks of the Foot by FastSCAN, Real-Time Imaging, 10(4), 2004, 217-228.
[11] Maekawa, T.; Wolter, E. E.; Patrikalakis, N. M.: Umbilics and Lines of Curvature for Shape interrogation, Computer Aided Geometric Design, 13, 1996, 133-161.
[12] Page, D. L.; Sun, Y.; Koschan, A. F.; Paik, J.; Abidi, M. A.: Normal Vector Voting: Crease Detection and Curvature Estimation on Large, Noisy Meshes, Graphical Models, 64, 2002, 199–229.
[13] Razdan, A.; Bae, M. S.: A hybrid approach to feature segmentation of triangle meshes, Computer-Aided Design, 35(9), 2003, 783-789.
[14] Subburaj, K.; Ravi, B.: High Resolution Medical Models and Geometric Reasoning starting from CT/MR Images, IEEE International Conference on CAD and Computer Graphics, Beijing, China, Oct. 15-18, 2007, 441-445.
[15] Viceconti, M.; Testi, D.; Simeoni, M.; Zannoni, C.: An Automated Method to Position Prosthetic Components within Multiple Anatomical Spaces, Computer Methods and Programs in Biomedicine, 70, 2003, 127-127.